Gradient-corrected *ab initio* calculations of spin-spiral states in fcc-Fe and the effects of the atomic-spheres approximation

M. Körling and J. Ergon
Theoretical Physics, Royal Institute of Technology, S-100 44 Stockholm, Sweden
(Received 7 June 1996)

The total energy of noncollinear spin-spiral states in bulk fcc-Fe is calculated using the linear-muffin-tin-orbital (LMTO) method in the atomic-spheres approximation (ASA). The relative stabilities of the spin-spiral states obtained with the gradient-corrected exchange-correlation functional PW91 differs from those of the local-spin-density approximation, but the discrepancy with experimental data remains. To analyze the accuracy of the LMTO-ASA, full-potential calculations using the linear-augmented-plane-wave method are also performed. The difference in magnetization energy between the methods is found to be comparable to the energy difference between the lowest-energy spin-spiral state and the lowest-energy collinear state, which is the antiferromagnetic state. [S0163-1829(96)51436-0]

The structural and magnetic properties of iron is a subject of continued great interest. Its location between antiferromagnetic and ferromagnetic regions in the periodic table allows for a variety of magnetic structures. In recent studies of thin Fe films grown epitaxially on Cu(001) several different magnetic structures are observed depending on growth conditions and film thickness.[1–3] Although the matter is still under debate, it seems clear that in the thickness range 6–10 ML the fcc phase is stable and shows an antiferromagnetic structure at low temperatures.[1] The fcc phase can also be stabilized as small clusters in a Cu matrix. The ground-state structure is found to be a noncollinear spiral-spin-density wave (SSDW).[4,5]

The close competition between different magnetic states has been confirmed by first-principles total-energy calculations for bulk fcc-Fe. Using density-functional theory[6] (DFT) in the local-spin-density approximation[7] (LSDA) the nonmagnetic (NM), ferromagnetic (FM), and antiferromagnetic (AF) states were shown to be close in energy, the relative stability depending sensitively on the atomic volume.[8,9] However, the LSDA fails to reproduce the ferromagnetic bcc phase as the ground state of bulk Fe. It has been shown in several studies that this problem can be overcome by including gradient corrections in the exchange-correlation functional.[10–13] We focus on PW91,[14,15] a generalized gradient-corrected functional constructed by Perdew and coworkers to satisfy most of the known conditions on the exact functional.

Extending DFT to the case of noncollinear magnetic structures, it was found that in bulk fcc-Fe some SSDW states have lower energy than the NM, FM, and AF states.[16–19] Recently, other noncollinear states were found with even lower energy using supercells.[20]

The purpose of this paper is, firstly, to investigate the effects of the gradient corrections on the energetics of the SSDW states. Secondly, since the treatment of noncollinearity relies on the use of the atomic-spheres approximation, we analyze the effect of this approximation by comparing with full-potential calculations for collinear states.

We have used the linear-muffin-tin-orbital (LMTO) method in the atomic-spheres approximation (ASA) to calculate the total energy of noncollinear SSDW configurations. The direction of the magnetic moment is taken to be constant inside each atomic sphere which means that a state with wave vector $\vec{q}$ is described by the spin density

$$\vec{m}(\vec{r}) = \sum_i H(|\vec{r}-\vec{r}_i|)m(|\vec{r}-\vec{r}_i|)\vec{e}_i,$$

$$\vec{e}_i = (\sin\theta\cos(\vec{q}\cdot\vec{r}_i), \sin\theta\sin(\vec{q}\cdot\vec{r}_i), \cos\theta),$$

where $\vec{r}_i$ are the lattice sites, $H(r)$ is a step function that equals one inside the ith atomic sphere and zero outside, and $\vec{e}_i$ is a unit vector in the direction of the ith magnetic moment. Moreover, we fix $\theta = \pi/2$.

It has been shown that the symmetry of configurations of this kind can be used to reduce the size of the needed unit cell,[21] in this case, to one atom. However, the size of the Hamiltonian matrix is doubled since majority and minority spins are no longer independent. We used the semirelativistic approximation for the valence electrons and the so-called combined correction term. The basis set consisted of s, p, d, and f functions and the $\vec{k}$ mesh contained 2744 points in the full Brillouin zone (BZ). Convergence test with 5832 points changed the total energy by less than 0.5 mRy. We used the PW91 subroutines[14,15] for both the the LSDA and the gradient-corrected calculations, in the former case with the nonlocal terms switched off. This LSDA functional yields results close to the Vosko-Wilk-Nusair parametrization[22] of the Ceperley-Alder data[23].

Figure 1 shows the total energy and the magnetic moment as functions of the spiral wave vector $\vec{q}$. The LSDA results (shown only for lattice constant $a = 6.80$ a.u.) are in good agreement with previous work[16–18] with minima occurring at around $\vec{q}_1 = (2\pi/a)(0,0,0.6)$, around $\vec{q}_2 = (2\pi/a)(0.5,0,1)$, and around $\vec{q}_3 = (2\pi/a)(0.25,0,0.5)$, with the first one being the lowest. For the PW91 the depths of the minima change so that the $\vec{q}_2$ spiral is slightly more stable than the $\vec{q}_1$. However, the PW91 does not improve the agreement with experimental data. The measured ground-state for small fcc-Fe clusters in a Cu matrix is a SSDW with $\vec{q}_m = (2\pi/a)(\delta,0,1)$, with $\delta \approx 0.1$.[4,5]

When using the LSDA, low-spin (LS) and high-spin (HS) states coexist in the region around the FM state, $\vec{q} = \Gamma$. No

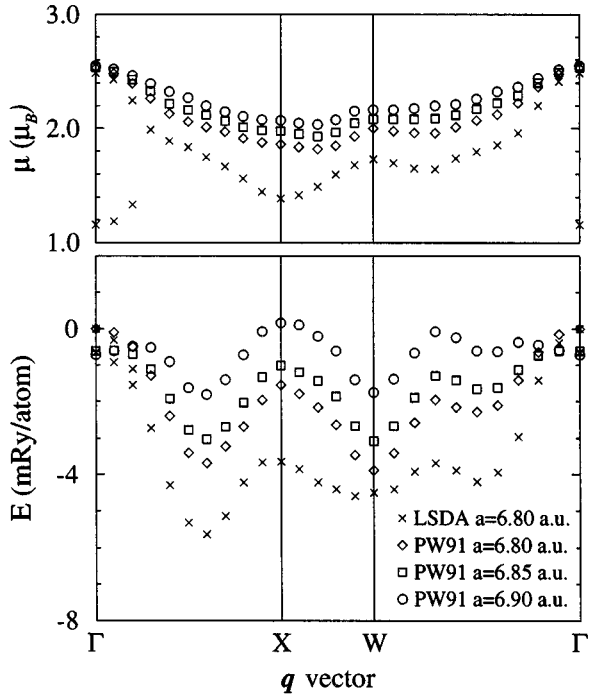

FIG. 1. Total energy and magnetic moment as functions of the spiral wave vector using the LMTO-ASA with the LSDA and the PW91. The energies are shown relative to the respective FM HS energies at $a=6.80$ a.u.

LS state was found using the PW91 for the lattice constants treated. The size of the HS magnetic moment for the FM is roughly the same using the LSDA and the PW91, but the PW91 shows less variation with the spiral wave vector.

Uhl, Sandratskii, and Kübler[18] showed that the stability of the $\vec{q}_1$ spiral state can be explained by the spin hybridization around the Fermi level. Figure 2 shows the LSDA band structure for the $\vec{q}_1$ and $\vec{q}_2$ spirals. The bands for the $\vec{q}_1$ spiral agree well with those in Ref. 18. At $\vec{k}=X$ the spin splitting opens up a gap stabilizing the spiral (see Ref. 18 for the unhybridized band structure) but for the $\vec{q}_2$ spiral the splitting is smaller, leaving bands crossing the Fermi level. In Fig. 3 we show the band structures for the PW91 case. The spin splitting is larger than for the LSDA for both $\vec{q}_1$ and $\vec{q}_2$ spirals. For the $\vec{q}_2$ spiral the majority states around $\vec{k}=L,\Gamma,X$ are pushed down below the Fermi level, thus stabilizing that spin-spiral state.

The volume dependences of the total energy and the magnetic moment for the NM, FM, and AF states and the $\vec{q}_1$ spiral state are shown in Fig. 4. The curves were obtained by fitting Murnaghan's equation of state to the calculated total energies. All of the LSDA data are known previously[9,19] and are included for reference. Gradient-corrected data for the NM, FM, and AF states have also been reported.[13,24] We now add to this picture the PW91 total energy curve of the $\vec{q}_1$ state. A corresponding curve was calculated for the $\vec{q}_2$ spiral and was found to lie on top of the $\vec{q}_1$ curve. In agreement with previous work[11,13] we make two observations. The PW91 favors larger atomic volumes and increases the magnetization energies. The expansion varies among the magnetic states from 2% for the NM state to 5% for the AF,

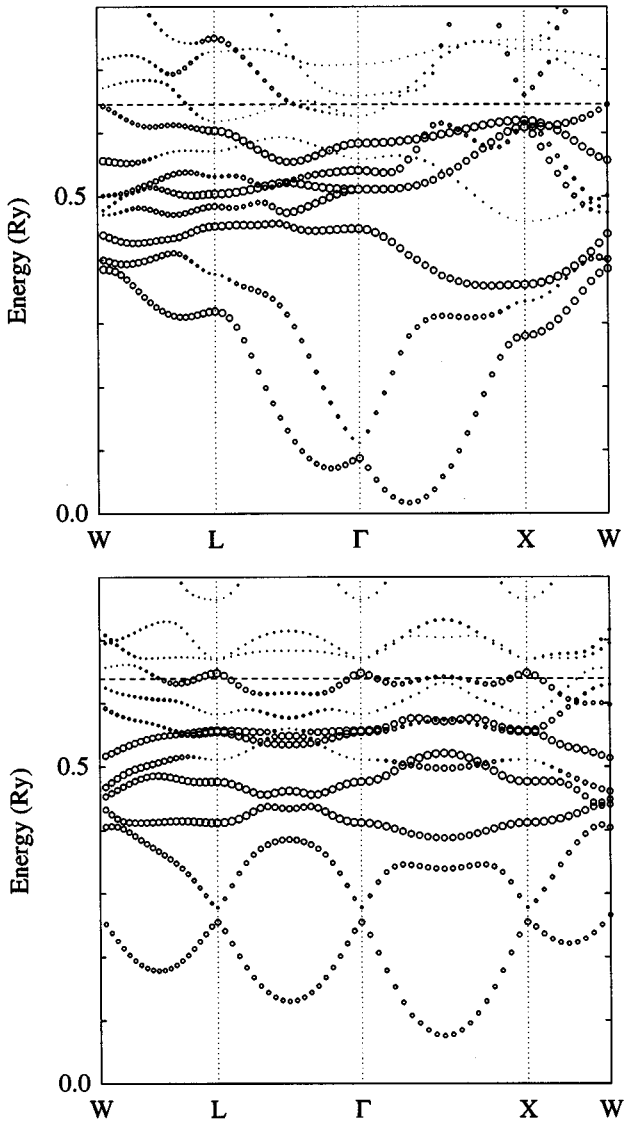

FIG. 2. The top and bottom panels show the LMTO-ASA LSDA band structures for wave vectors $\vec{q}_1=(2\pi/a)(0,0,0.6)$ and $\vec{q}_2=(2\pi/a)(0.5,0,1)$, respectively. An eigenstate is represented by a circle with the center at the eigenenergy and the radius proportional to the spin character of the state. Large circles correspond to majority-spin states.

$\vec{q}_1$, and $\vec{q}_2$ states. The change in magnetization energy also varies, even between the AF and the $\vec{q}_1$ states, that are expanded by roughly the same amount. This shows that the effect of the gradient corrections is not that of a pure volume expansion.

We interpret the irregularity in the PW91 data at $a\approx 6.78$ a.u. as an indication of a ferrimagnetic state. Since our ASA calculations involve only one atom per unit cell, they are effectively constrained so that the magnetic moments in, e.g., the AF state, must be opposite in direction but equal in magnitude. A ferrimagnetic state has been reported[25] and is also seen in our full-potential calculations below.

Previous work has shown that for the structural properties of nonmagnetic transition metals, the ASA introduces errors of the same magnitude as the difference between the LSDA and the PW91.[26] To check if the same is true for magnetic

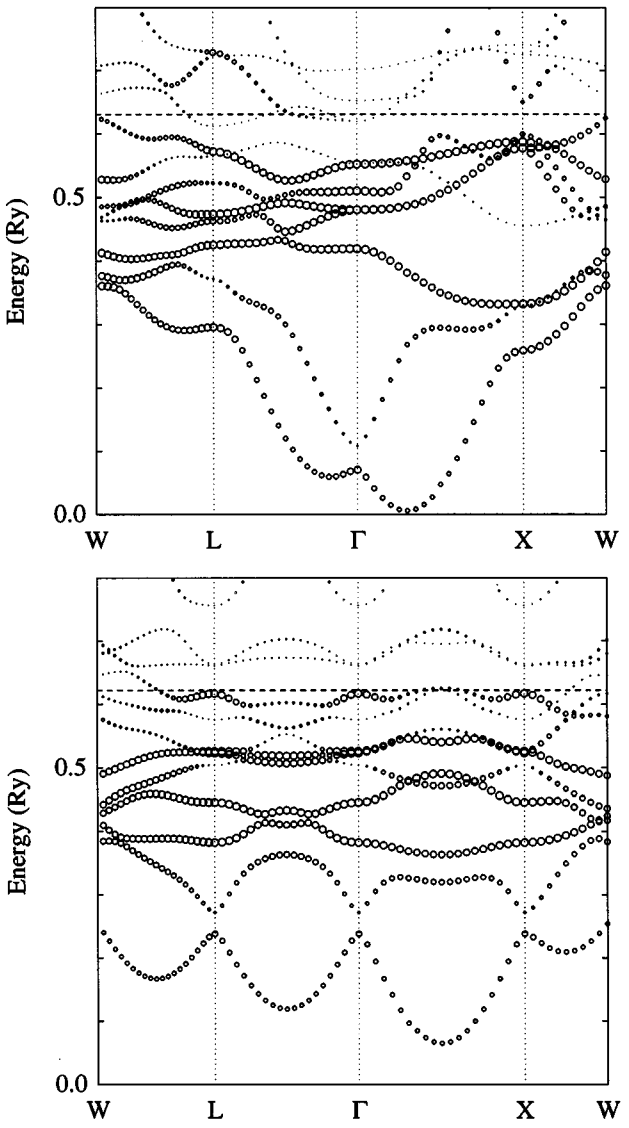

FIG. 3. The top and bottom panels show the LMTO-ASA PW91 band structures for wave vectors $\vec{q}_1=(2\pi/a)(0,0,0.6)$ and $\vec{q}_2=(2\pi/a)(0.5,0,1)$, respectively. For explanations, see Fig. 2.

properties, calculations with no shape approximation were performed for the NM, FM, and AF states. These calculations employed the full-potential (FP) linear-augmented-plane-wave (LAPW) method.[27] The $\vec{k}$ mesh consisted of 4000 points in the full BZ and the number of plane waves used in the interstitial region was determined by the condition $k_{\max}R_{\mathrm{MT}}=10$. For all structures a cell containing two atoms was used.

In Fig. 5 the volume dependences of the total energy and the magnetic moment are shown for the LSDA and the PW91, again using Murnaghan's equation of state. The LSDA results are in good agreement with previous work.[8] In the PW91 case we note the presence of a LS FM state and a ferrimagnetic variation of the AF state in the region $a\approx 6.7$ a.u. to $a\approx 6.8$ a.u.

Comparing the results of the LMTO-ASA and FP-LAPW calculations, i.e., Figs. 4 and 5, we note two differences. First, as observed earlier,[26,28] the ASA method gives consistently larger equilibrium lattice constants than the FP method. Second, within the PW91, the magnetization ener-

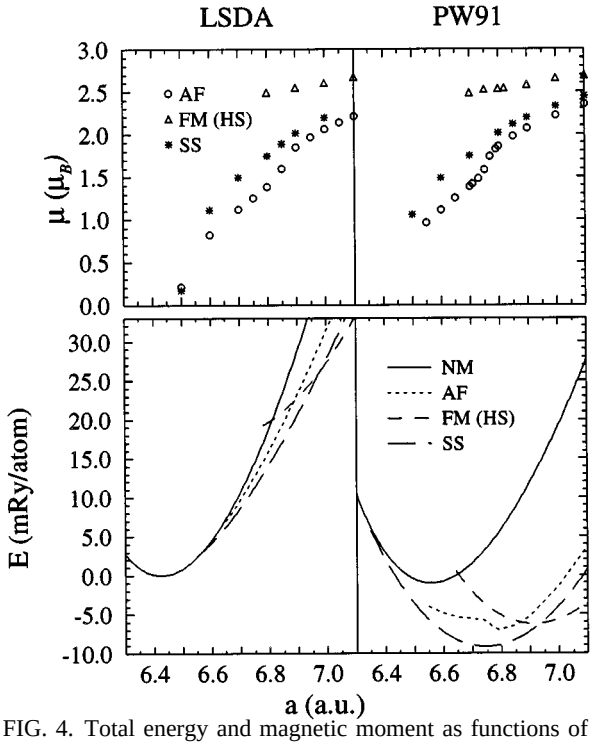

FIG. 4. Total energy and magnetic moment as functions of the lattice constant using the LMTO-ASA together with the LSDA and the PW91. The symbol SS denotes the $\vec{q}_1$ spiral in the LSDA case and both $\vec{q}_1$ and $\vec{q}_2$ states in the PW91 case. The energies are shown relative to the respective NM equilibrium energies.

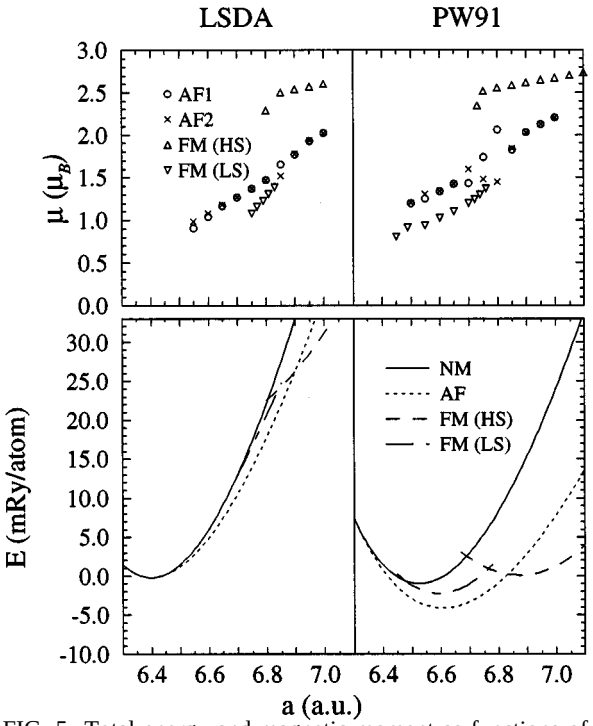

FIG. 5. Total energy and magnetic moment as functions of the lattice constant using the FP-LAPW together with the LSDA and the PW91. The energies are shown relative to the respective NM equilibrium energies. AF1 and AF2 denotes the magnitude of the magnetic moments on the inequivalent sites.

gies are overestimated by the LMTO-ASA. For example, at fixed lattice constant $a=6.80$ a.u., the FM-NM energy difference is 11 mRy for the LMTO-ASA and 8 mRy for the FP-LAPW. This change is smaller than the increase in magnetization energy caused by the gradient corrections but it is not negligible.

To further analyze the difference between the LMTO-ASA and the FP-LAPW, we carried out additional FP-LAPW calculations using the so-called warped-muffin-tin approximation,[29] i.e., allowing only spherically symmetric terms in the charge density inside the muffin tin spheres. Figure 6 shows how the total energy curves are changed by this constraint (for the PW91 case only). The effect is strongest on the AF state, while the NM state is almost unchanged. For both AF and FM states the magnetization energies are not changed towards the LMTO-ASA results, but are instead decreased. This suggests that the overestimation of the magnetization energies by the LMTO-ASA is due to the overlapping-spheres treatment of the interstitial region. However, we note that there are other differences between the LMTO-ASA and the FP-LAPW than the approximations defined by the ASA.

In conclusion, we have shown, using the LMTO-ASA, that gradient corrections change the relative stabilities of the SSDW states but that the discrepancy with experimental data remains. Furthermore, the LMTO-ASA is shown to introduce errors in the magnetization energies that are of the same order of magnitude as the relative stability between the lowest-energy SSDW state and the AF state, which is the lowest-energy collinear state. This deficiency of the LMTO-ASA can be of importance in the recent[30,20] finite-temperature spin-dynamics applications of DFT.

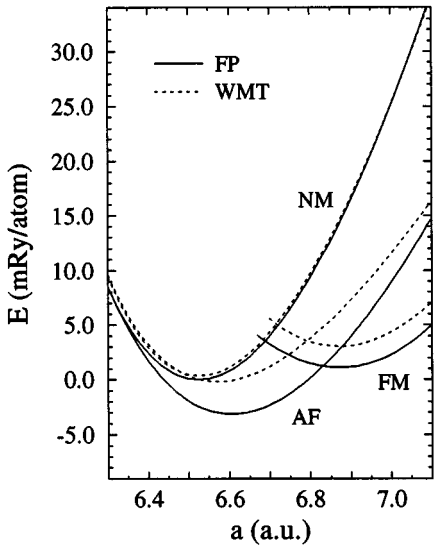

FIG. 6. Total energy and magnetic moment as functions of the lattice constant using the PW91 with the FP-LAPW and the warped-muffin-tin approximation (WMT) (see text). The energies are shown relative to the FP NM equilibrium energy.

We wish to thank J. Perdew for providing the PW91 subroutines and L. Sandratskii for helpful discussions. This work has been supported by the Swedish research councils NUTEK and NFR.

[1] R. D. Ellerbrock, A. Fuest, A. Schatz, W. Keune, and R. A. Brand, Phys. Rev. Lett. **74**, 3053 (1995).
[2] S. Müller, P. Bayer, C. Reischl, K. Heinz, B. Feldmann, H. Zillgen, and M. Wuttig, Phys. Rev. Lett. **74**, 765 (1995).
[3] Dongqi Li, M. Freitag, J. Pearson, Z. Q. Qiu, and S. D. Bader, Phys. Rev. Lett. **72**, 3112 (1994).
[4] Y. Tsunoda, J. Phys. C **1**, 10 427 (1989).
[5] Y. Tsunoda, Y. Nishioka, and R. M. Nicklow, J. Magn. Magn. Mater. **128**, 133 (1993).
[6] P. Hohenberg and W. Kohn, Phys. Rev. B **136**, 864 (1964); W. Kohn and L. J. Sham, Phys. Rev. A **140**, 1133 (1965).
[7] L. Hedin and B. I. Lundqvist, J. Phys. C **4**, 2064 (1971).
[8] C. S. Wang, B. M. Klein, and H. Krakauer, Phys. Rev. Lett. **54**, 1852 (1985).
[9] V. L. Moruzzi, P. M. Marcus, and J. Kübler, Phys. Rev. B **39**, 6957 (1989).
[10] P. Bagno, O. Jepsen, and O. Gunnarsson, Phys. Rev. B **40**, 1997 (1989).
[11] D. J. Singh, W. E. Pickett, and H. Krakauer, Phys. Rev. B **43**, 11 628 (1991).
[12] T. C. Leung, C. T. Chan, and B. N. Harmon, Phys. Rev. B **44**, 2923 (1991).
[13] T. Asada and K. Terakura, Phys. Rev. B **46**, 13 599 (1992).
[14] J. P. Perdew, in *Electronic Structure of Solids 1991*, edited by P. Ziesche and H. Eschrig (Akademie Verlag, Berlin, 1991), Vol. 11.
[15] J. P. Perdew, K. Burke, and Y. Wang (unpublished).
[16] O. N. Myrasov, A. I. Liechtenstein, L. M. Sandratskii, and V. A. Gubanov, J. Phys. C **3**, 7683 (1991).
[17] O. N. Myrasov, V. A. Gubanov, and A. I. Liechtenstein, Phys. Rev. B **45**, 12 330 (1992).
[18] M. Uhl, L. M. Sandratskii, and J. Kübler, J. Magn. Magn. Mater. **103**, 314 (1992).
[19] M. Uhl, L. M. Sandratskii, and J. Kübler, Phys. Rev. B **50**, 291 (1994).
[20] V. P. Antropov, M. I. Katsnelson, B. N. Harmon, M. van Schilfgaarde, Phys. Rev. B **54**, 1019 (1996).
[21] L. M. Sandratskii and P. G. Guletskii, J. Phys. F **16**, L43 (1986).
[22] S. H. Vosko, L. Wilk, and M. Nusair, Can. J. Phys. **58**, 1200 (1980).
[23] D. M. Ceperley and B. J. Alder, Phys. Rev. Lett. **45**, 566 (1980).
[24] J. Häglund, Phys. Rev. B **47**, 566 (1993).
[25] Y. Zhou, W. Zhang, L. Zhoung, and D. Wang, J. Magn. Magn. Mater. **145**, L273 (1995).
[26] V. Ozoliņš and M. Körling, Phys. Rev. B **48**, 18 304 (1993).
[27] P. Blaha, K. Schwarz, P. Dufek, and R. Augustyn, WIEN95 (Techical University of Vienna, Vienna, 1995). [Improved and updated Unix version of the original copyrighted WIEN-code, which was published by P. Blaha, K. Schwarz, P. Sorantin, and S. B. Trickey, in Comput. Phys. Commun. **59**, 399 (1990)].
[28] K. B. Hathaway, H. J. F. Jansen, and A. J. Freeman, Phys. Rev. B **31**, 7603 (1985).
[29] H. J. F. Jansen and S. S. Peng, Phys. Rev. B **37**, 2689 (1988).
[30] V. P. Antropov, M. I. Katsnelson, M. van Schilfgaarde, and B. N. Harmon, Phys. Rev. Lett. **75**, 729 (1995).